J. Mountain Res. P-ISSN: 0974-3030, E-ISSN: 2582-5011 DOI: https://doi.org/10.51220/jmr.v20-i2.23
Vol. 20(2), (2025), 195-206

Green Synthesis of Zinc Oxide Nanoparticles using *Malva parviflora* Leaf Extract: A Comprehensive Study on its Characterization, Antioxidant, and Antimicrobial Efficacy

Vipul* • Goutam Kumar • P.P. Badoni

Chemistry Department, H.N.B. Garhwal University B.G.R. Campus, Pauri-246001, Uttarakhand

*Corresponding Author's email Id: parth25797@gmail.com

Received: 7.10.2025; Revised: 7.12.2025; Accepted: 8.12.2025
©Society for Himalayan Action Research and Development

Abstract: This study presents an eco-friendly and sustainable approach for synthesizing zinc oxide nanoparticles (ZnO NPs) using an aqueous leaf extract of *Malva parviflora* as a reducing and stabilizing agent. The synthesis involved the reaction of 0.1 M zinc acetate with the plant extract under alkaline conditions (pH 10–12), resulting in the formation of a white precipitate indicative of ZnO nanoparticle formation. The biosynthesized nanoparticles were comprehensively characterized using multiple analytical techniques. UV-Vis spectroscopy confirmed the formation of ZnO NPs with an absorption peak at 314 nm. X-ray diffraction (XRD) analysis revealed a hexagonal wurtzite crystal structure with an average crystallite size of approximately 25 nm. Fourier transform infrared (FTIR) spectroscopy identified proteins, polysaccharides, and phenolic compounds from the leaf extract as capping agents responsible for nanoparticle stabilization. Electron microscopy (SEM and TEM) showed polycrystalline particles ranging from 15 to 50 nm, forming larger aggregates. Dynamic light scattering (DLS) indicated a hydrodynamic diameter of 693.5 nm with moderate polydispersity (PDI: 0.352). The biosynthesized ZnO NPs exhibited significant dose-dependent antioxidant activity in the DPPH assay (IC_{50} = 660.74 µg/mL) and demonstrated potent antibacterial efficacy against *Staphylococcus aureus* (zone of inhibition: 13.83–14.93 mm) with selective antifungal activity. These findings highlight the potential of *M. parviflora*-mediated ZnO NPs as promising candidates for biomedical applications, including antimicrobial therapies and antioxidant formulations.

Keywords: *Malva parviflora* • Zinc oxide nanoparticles • Biomedical applications.

Introduction

Nanoparticles, typically sized between 1 and 100 nm, possess distinctive physicochemical properties arising from their high surface area–to–volume ratio, making them significantly different from bulk materials. Zinc oxide nanoparticles (ZnO-NPs) are particularly noteworthy due to their biocompatibility, thermal stability, non-toxicity, cost-effectiveness, and strong ultraviolet (UV) absorption capacity (Abdullah et al., 2020; Chauhan et al., 2020; Espitia et al., 2012; Şahin et al., 2021). These attributes have broadened their applications across medicine, agriculture, environmental remediation, food packaging, and solar energy sectors (Galstyan et al., 2015; Hrishikesh Upadhyaya et al., 2018; Miri et al., 2020).

Traditional ZnO-NP synthesis techniques often rely on physical and chemical procedures, which, although efficient, raise environmental and safety concerns due to hazardous reagents and toxic by-products (Ganesh Saratale et al., 2018; Iravani, 2011; Javidan et al., 2015; Kumar et al., 2009). These limitations have accelerated interest in green or biological synthesis approaches that use microorganisms and plants as eco-friendly, economical, and sustainable alternatives (Iqbal et al., 2021; Kesharwani et al., 2009; Makarov et al., 2014; Mittal et al., 2013; Noah, 2019).

Plant-mediated green synthesis has emerged as a particularly promising route, utilizing phytochemicals such as flavonoids, phenols, alkaloids, proteins, and antioxidants as natural reducing and capping agents to form stable

nanoparticles under mild, non-toxic conditions (Akhtar et al., 2013; Huang et al., 2007; Ijaz et al., 2020; Li et al., 2007; Li et al., 2011; Malik et al., 2014; Mukunthan & Balaji, 2012). This method minimizes environmental risks, lowers energy demands, and enhances the biological compatibility and functional activity of the resulting nanoparticles (Devatha & Thalla, 2018; Iqbal et al., 2020; Zhao et al., 2012). The phytochemical richness of plants also enables better control over nanoparticle morphology, providing advantages over microbial synthesis.

Malva parviflora Linn., or cheeseweed, is a medicinal plant known for potent antioxidant, antimicrobial, antifungal, and antidiabetic properties owing to its high levels of flavonoids, rutin, tannins, polyphenols, and alkaloids (Abd-El-Rahim-Mashaly, 2012; Al-Qarawi & Al-Obaidi, 2018; Farhan et al., 2012; Forouzanfar et al., 2014; Shehata & Galal, 2014; Singh & Navneet, 2017). These bioactive molecules also act as effective natural reductants and stabilizers in nanoparticle formation (Murray et al., 1982; Raliya et al., 2015).

This study aims to establish a simple, green synthesis protocol for ZnO-NPs using Malva parviflora leaf extract, characterize the nanoparticles, and evaluate their antimicrobial, antioxidant, and other biological activities to identify potential biomedical and environmental applications.

Materials and Methods

Identification and Preparation of Plant Extract: Fresh *Malva parviflora* plants were collected during their flowering stage from the Garhwal Himalayan region from Uttarkashi in Uttarakhand, India.The plant species was identified and authenticated by the Department of Botany, Hemwati Nandan Bahuguna Garhwal University (HNBGU). A voucher specimen was deposited in the university herbarium, and the accession number **GUH20836** was assigned for future reference. The leaves were washed thoroughly, shade-dried for 10–15 days, and then ground into a fine powder. Subsequently, 20 g of this leaf powder was boiled in 200 mL of distilled water at 80°C for 30 minutes. After cooling to room temperature, the mixture was filtered through Whatman No. 1 filter paper to obtain a clear aqueous extract. This extract was stored at 4°C and subsequently utilized as the reducing and capping agent for the biosynthesis of ZnO nanoparticles.

Synthesis of ZnO Nanoparticles: A 200 mL aliquot of 0.1 M zinc acetate dihydrate ($Zn(CH_3COO)_2 \cdot 2H_2O$) solution was magnetically stirred at 60°C for 30 minutes. Subsequently, 200 mL of freshly prepared Malva parviflora leaf extract was added dropwise to the reaction mixture. The pH was gradually adjusted to 10–12 using 1 M NaOH to ensure efficient precipitation of zinc oxide. Formation of a milky white precipitate indicated successful synthesis of ZnO nanoparticles. The precipitate was isolated by centrifugation at 5000 rpm for 20 minutes, then washed three times with distilled water and once with acetone to remove residual ionic and organic impurities. The purified product was dried in a hot air oven at 80°C for 6–8 hours, ground into a fine powder, and stored in airtight vials in a cool, dry, and dark place until further characterization and analysis.

Characterization of ZnO-NPs: The biosynthesized ZnONPs were characterized morphologically, physically, and chemically using various analytical techniques. The formation of zinc ions to ZnONPs was determined by measuring the absorption spectra of reaction solutions via UV-4000 UV-Vis spectrophotometer (LABTRONICS LT-2201) between 200–700 nm. The morphology of the ZnONPs was analyzed through SEM (Carl Zeiss, EVO18 − applied with EDX detectors). TEM analyses (JEOL JEM-F200) was performed to study size and shape of ZnONPs. The average particle size and particle size distribution of ZnONPs were studied via DLS system(Malvern PANalytical, ZETASIZER PRO). FTIR (Thermo Fisher,

Nicolet Summit X) analysis was performed between 500–4500 cm^{-1} to study diverse types of functional groups which are responsible fordevelopment and effective stabilizations for ZnONPs using various modes of vibrations. The crystalline structure of biogenic ZnONPs was determined by XRD (Malnvern PANanalytical, Empirian) and crystal size was calculated.

Bio-Potentials of ZnO NPs

Antioxidant Activity: The free radical scavenging activity was evaluated using the DPPH (2,2-diphenyl-1-picrylhydrazyl) assay. Ascorbic acid was used as a standard.

Antimicrobial Activity: The well diffusion method was employed against Gram-positive *Staphylococcus aureus* **(MTCC 452)**, Gram-negative *Escherichia coli* **(MTCC452)**, and the fungi *Trichoderma reesei* **(MTCC 164)** and *Aspergillus niger* **(MTCC282).** Zones of Inhibition (ZOI) were measured after 24h of incubation at 37°C.

Results and Discussion

UV-Vis Spectroscopy: The UV-Vis absorption spectrum of the synthesized ZnONPs (Fig.1) exhibited absorption peak at approximately 314 nm. This blue-shifted peak relative to bulk ZnO absorption (~370 nm)(Song et al., 2011) is consistent with the quantum confinement effect arising from the reduced particle size and altered electronic band structure.(Ahmed & Edvinsson, 2020). The clean baseline after the absorption edge indicates a stable colloidal suspension, with the phytochemicals from *Malva parviflora* providing effective stabilizing and capping during synthesis(Sulak, 2021). These optical features confirm the formation and stability of ZnO nanoparticles with size-dependent properties(Ahmed & Edvinsson, 2020; Sulak, 2021).

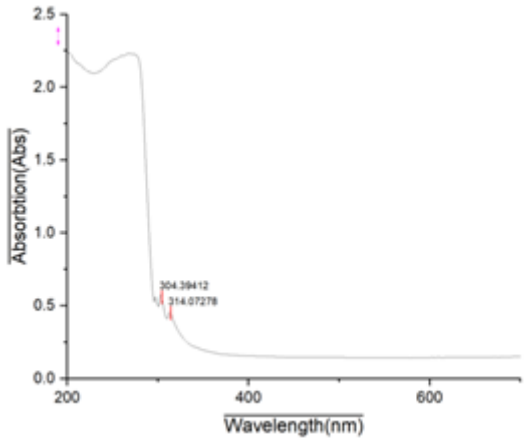


Fig 1: UV-Vis absorption spectrum of the synthesized ZnO NPs

X-ray Diffraction (XRD) Analysis

The XRD pattern (Fig.2)displayed well-defined diffraction peaks that matched the hexagonal wurtzite crystal structure of ZnO, with characteristic reflections at 2θ values approximately 31.7°, 34.4°, 36.2°, 47.5°, 56.6°, 62.8°, 66.3°, 67.9°, and 69.1°. The absence of additional peaks confirmed the high purity of the synthesized nanoparticles. The average crystallite size, determined using the Scherrer equation from the (101) peak(Mustapha et al., 2019), was approximately 25 nm, confirming the nanoscale nature of the ZnO particles. Such crystallinity is crucial for defining their physicochemical and functional properties(Le Nhat Trang et al., 2023; Wang, 2004).

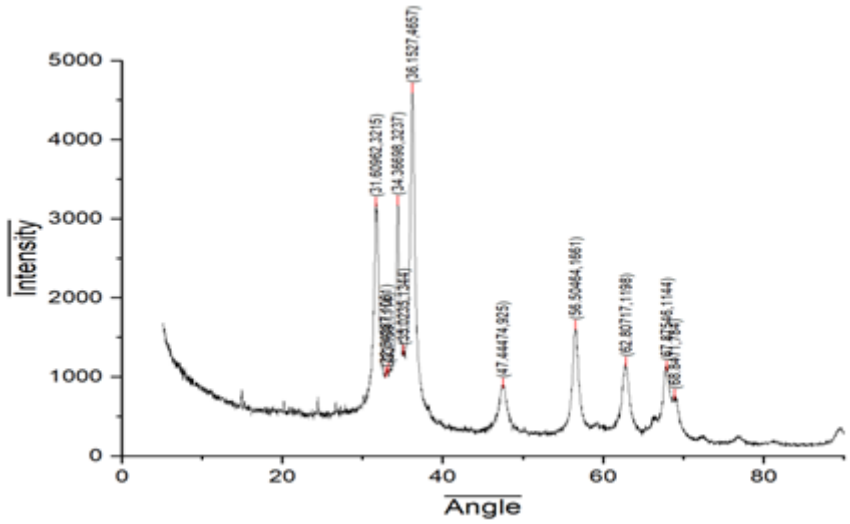


Fig 2: XRD pattern of the synthesized ZnO NPs

Fourier-Transform Infrared (FTIR) Spectroscopy

FTIR spectra(Fig.3) revealed several prominent absorption bands related to biomolecules capping the ZnO nanoparticles. The broad band near 3350 cm^{-1} may be attributed to O–H stretching vibrations of hydroxyl groups and adsorbed water(Cheperli et al., 2024; Sulak, 2021). The peaks between 1400–1600 cm^{-1} assumed to be corresponding C=O and amide group vibrations, indicating proteins and flavonoids binding from plant extract. Importantly, a strong absorption band below 600 cm^{-1} confirmed the Zn–O stretching vibration, verifying ZnO nanoparticle formation. These findings illustrate the role of plant phytochemicals as natural capping and stabilizing agents enhancing particle stability (Cheperli et al., 2024; Sulak, 2021).

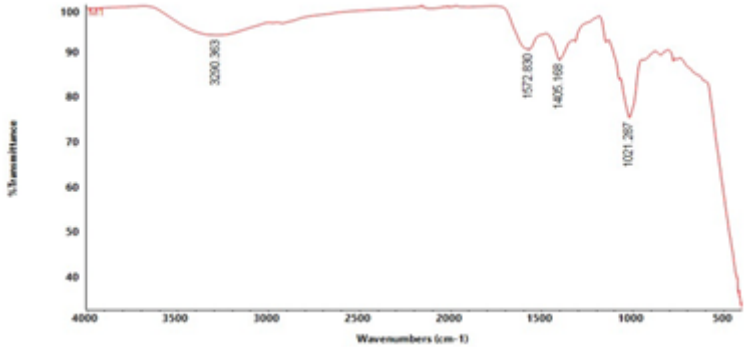


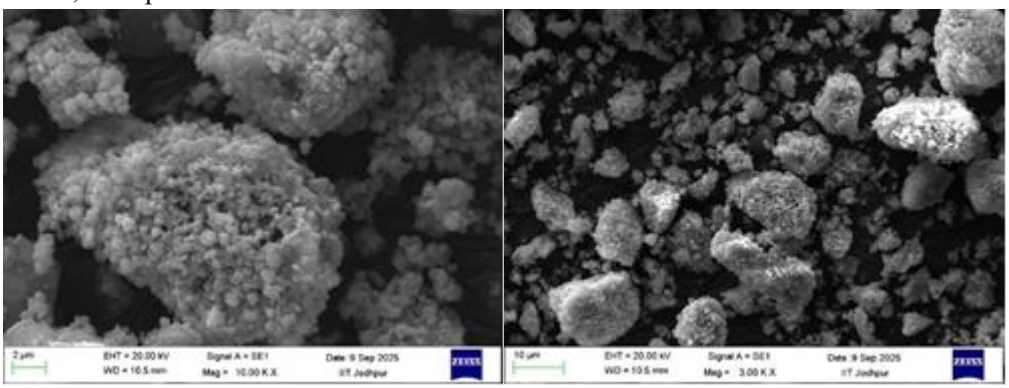
Fig 3: FTIR spectrum of the synthesized ZnO NPs

Electron Microscopy (SEM and TEM) Analysis

SEM analysis revealed that the biosynthesized ZnO nanoparticles form polydisperse, micro-scale aggregates ranging from sub-micron to several micrometers in diameter (Fig.4a,4b). The aggregates exhibited spherical to cauliflower-like morphology with characteristic rough surface texture and porous architecture. Higher magnification images confirmed that these macro-structures are composed of smaller primary nanoparticles, with individual particle sizes ranging from 20-85 nm as determined by ImageJ analysis(Singh et al 2018).

The observed aggregation pattern and surface morphology are consistent with green synthesis mechanisms, where phytochemical capping agents promote the formation of complex supramolecular assemblies(Singh et al., 2018). The aggregation state visualized in SEM correlates well with the larger

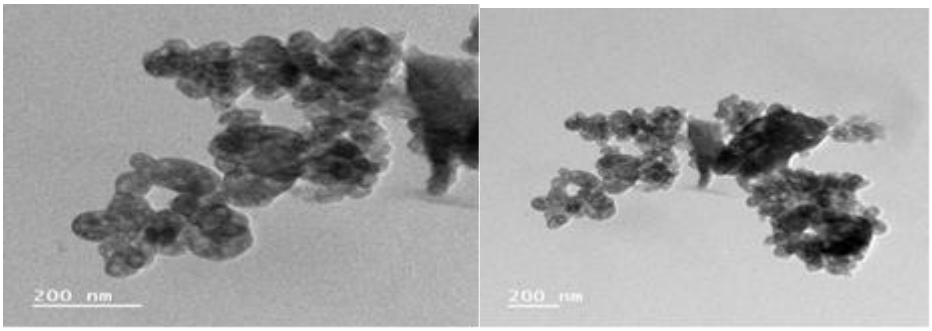
hydrodynamic diameter (694 nm) measured by DLS, with the expected discrepancy arising from sample preparation differences - SEM analyzes dried, collapsed structures while DLS measures hydrated aggregates in suspension(Bhattacharjee, 2016; Tomaszewska et al., 2013).



(4a) **(4b)**

Fig 4a, 4b. SEM images of the synthesized ZnO NPs

TEM analysis provided high-resolution insight into the primary nanostructure of the biosynthesized ZnO nanoparticles (Fig.5a,5b). The micrographs revealed that the micro-scale aggregates observed in SEM consist of smaller, primary nanoparticles with a size range of 15–40 nm as determined by ImageJ analysis, showing excellent agreement with the crystallite size (~25 nm) determined by XRD analysis.



(5a) **(5b)**

Fig 5a, 5b. TEM images of the synthesized ZnO NPs

The primary particles exhibited predominantly spherical morphology with a tendency to form chain-like agglomerates. The consistent discrepancy between TEM particle size and XRD crystallite size indicates the polycrystalline nature of the nanoparticles, where each visible particle comprises multiple smaller crystalline domains.High-resolution TEM (HRTEM) imaging confirmed the crystalline structure, revealing distinct lattice fringes with an interplanar spacing of 0.26 nm corresponding to the (002) plane of hexagonal wurtzite ZnO, thereby validating the crystalline phase identified by XRD (Wang, 2004).

Dynamic Light Scattering (DLS)

DLS analysis (Fig.6) reported an average hydrodynamic diameter (Z-average) of 693.5 nm with a polydispersity index (PDI) of 0.35, indicating moderate size distribution and some degree of aggregation in aqueous suspension(Bhattacharjee, 2016). The hydrodynamic size exceeds the crystalline size derived from XRD due to organic coating and possible nanoparticle agglomeration, common in green-synthesized samples with surface-bound biomolecules(Abdelbaky et al., 2022).

These results emphasize the importance of surface chemistry in nanoparticle behavior in colloidal systems (Abdelbaky et al., 2022; Bhattacharjee, 2016).

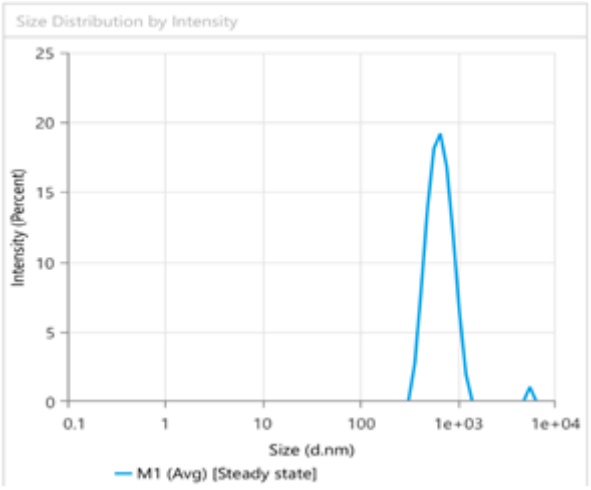


Fig 6: DLS Graph of synthesizedZnO NPs

Zeta potential measurements yielded an average value of -11.95 mV with a deviation of 7.15 mV. This moderately negative zeta potential suggests partial electrostatic repulsion among nanoparticles, imparted by phytochemical capping, contributing to colloidal stability (Hussien et al., 2025; Jose & Shinde, 2024). Although higher magnitude potentials (more negative than -30 mV) typically indicate strong stability, the measured value implies a stable yet moderately aggregating suspension, consistent with the DLS findings (Jose & Shinde, 2024).

The overall physicochemical profile of ZnO nanoparticles synthesized via *Malva parviflora* leaf extract emerges from the complementary insights of ZnO nanoparticles displayed a blue-shifted UV–Vis absorption peak at 314 nm, indicating reduced particle size and strong quantum confinement. XRD confirmed the hexagonal wurtzite phase with a crystallite size of about 25 nm, consistent with nanoscale formation. FTIR spectra showed Zn–O stretching below 600 cm^{-1} and functional groups (O–H, C=O, amide) from plant phytochemicals, verifying green synthesis and surface capping. SEM and TEM images revealed mostly spherical to irregular aggregates (15–85 nm subunits), while DLS indicated a larger hydrodynamic diameter (~693.5 nm) due to aggregation and hydration. The polydispersity index (0.35) reflected moderate size variation. A zeta potential of −11.95 mV suggested fair colloidal stability from phytochemical capping, though partial clustering occurs. Overall, the data show effective green synthesis yielding crystalline, moderately stable ZnO nanoparticles with biomolecular surface modification.

Biological Activities

Antioxidant Activity

The antioxidant potential of ZnO nanoparticles synthesized using *Malva parviflora* (leaf extract) was evaluated by the DPPH radical scavenging assay. *Malva Parviflora* leaf extract exhibited a concentration-dependent free radical scavenging activity (%RSA) ranging from approximately 27% at 62.5 µg/mL to 62% at 1000 µg/mL. The half-maximal inhibitory concentration (IC_{50}) was calculated to be 660.74 ± 2.15 µg/mL, indicating moderate antioxidant capacity.

For comparison, the standard antioxidant ascorbic acid showed an IC_{50} of 18.09 ± 0.51 µg/mL, confirming its stronger radical quenching ability at lower concentrations(Kedare & Singh, 2011). The observed antioxidant activity of *Malva Parviflora* leaf extract can be attributed to the

phytochemical constituents present on the nanoparticle surface, which effectively donate electrons or hydrogen atoms to neutralize DPPH radicals.(Baliyan et al., 2022).

Although *Malva parviflora* leaf extract displayed relatively moderate antioxidant efficiency compared to pure ascorbic acid, these results demonstrate that the biosynthesized ZnO nanoparticles possess significant radical scavenging capability. This property supports their potential use in biomedical and food preservation applications where mitigation of oxidative stress is critical.

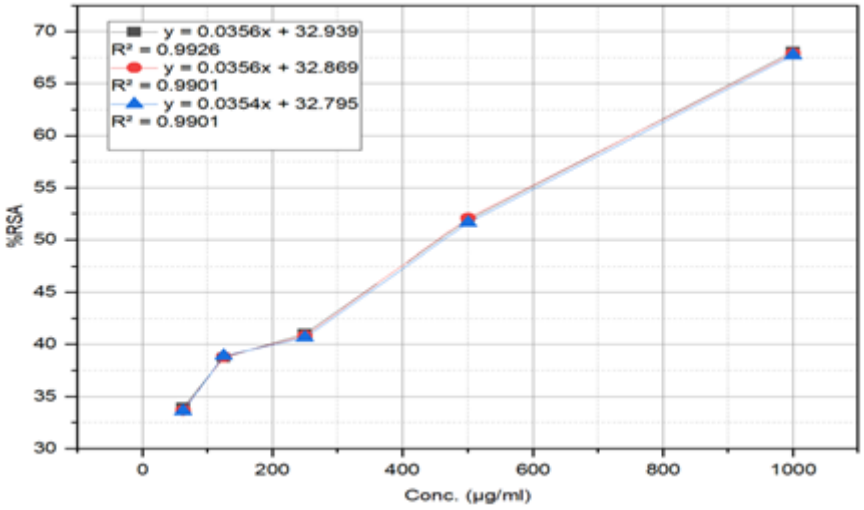


Fig 7: Antioxidant potential of ZnONPs.

The biosynthesized ZnO nanoparticles exhibited a concentration-dependent antioxidant activity in the DPPH assay (Fig.7). A strong linear correlation between concentration and radical scavenging activity was observed across all replicates ($R^2 \geq 0.99$), confirming the dose-responsive efficacy and high reproducibility of the antioxidant effect.

Antimicrobial Activity

Antimicrobial and Antifungal Activity of Biosynthesized ZnO Nanoparticles (Malva Parviflora leaf extract)

The antimicrobial potential of ZnO nanoparticles synthesized via *Malva parviflora* was evaluated against representative bacterial and fungal strains using the well diffusion method. The bacteria tested included *Staphylococcus aureus* (Gram-positive) and *Escherichia coli* (Gram-negative), while antifungal activity was assessed against *Trichoderma reesei* and *Aspergillus niger*.

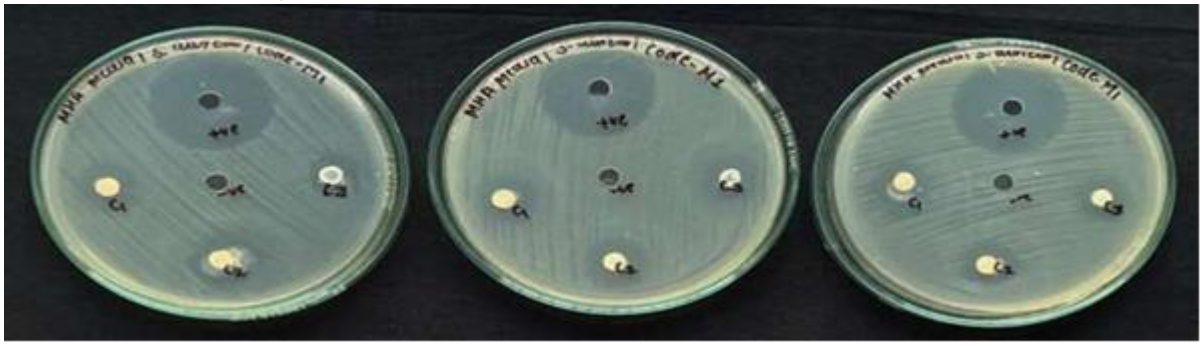


Fig8. Antibacterial activity of sample *Malva parviflora* of concentrations:100mg/ml,50mg/ml and 25mg/ml,against*S. aureus* using well diffusion method; +vecontrol–Ciprofloxacin used at100ppm, -ve control Methanol.

At concentrations of 100, 50, and 25 mg/mL, *Malva Parviflora* leaf extract exhibited significant antibacterial activity against *S. aureus*, with mean zones of inhibition measuring approximately 13.8 mm, 14.9 mm, and 14.0 mm, respectively. These inhibition zones indicate substantial efficacy, though less than the positive control ciprofloxacin, which showed an average zone of approximately 30.2 mm. The test also revealed moderate activity against *E. coli*, with zones of inhibition at 12.5 mm, 12.3 mm, and 11.6 mm across the tested concentrations. The negative control (methanol) displayed no antibacterial activity, ensuring that the observed effects were attributable to the nanoparticles.

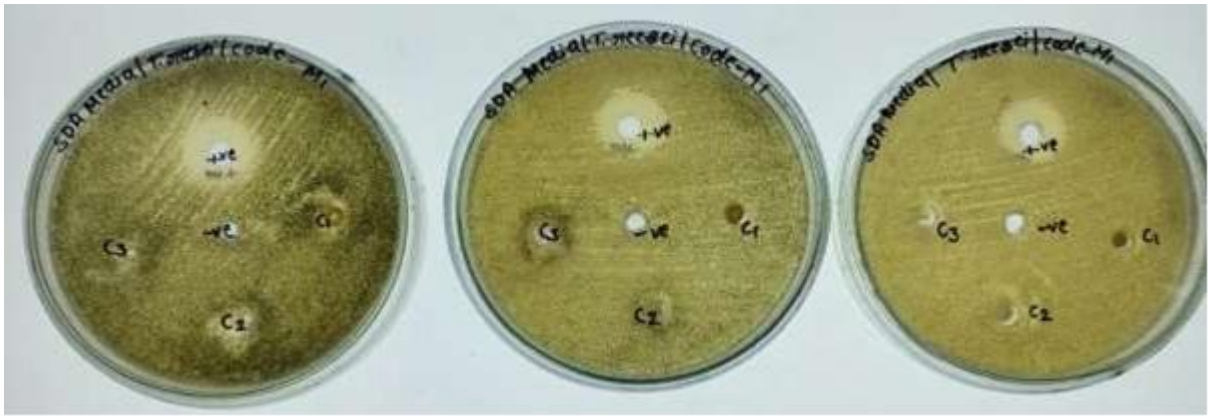


Fig 9. Antifungal activity of sample *Malva parviflora* of concentrations :100mg/ml, 50mg/ml and 25mg/ml, against *T.reesei*using well diffusion method; +vecontrol–Itraconazole used at 300ppm, -ve control Methanol

Malva Parviflora leaf extract demonstrated antifungal efficacy against *T. reesei*, yielding inhibition zones of 9.3 mm, 7.8 mm, and 7.1 mm at 100, 50, and 25 mg/mL concentrations, respectively. Though lower than the antifungal drug itraconazole (~14.3 mm zone), these results confirm the antifungal potential of the synthesized nanoparticles. However, no significant inhibition was observed against *A. niger*, with zero zones of inhibition reported, contrasting with itraconazole control (~16.5 mm).

The green synthesized ZnO nanoparticles exhibited stronger antibacterial activity against Gram-positive *S. aureus* relative to Gram-negative*E. coli*, aligning with known differences in bacterial cell wall structure influencing nanoparticle penetration and efficacy (Babayevska et al., 2022; Mendes et al., 2022). The moderate antifungal activity against T. reesei but not A. niger suggests selectivity or differential sensitivity among fungal species(Subba et al., 2024). The concentration-dependent activity and absence of effect in negative controls confirm the intrinsic antimicrobial properties of the biosynthesized ZnO nanoparticles. The presence of phytochemical capping from Malva parviflora may contribute to enhanced biocompatibility and sustained nanoparticle action (Al-Hamad et al., 2025).

These findings highlight the applicability of eco-friendly ZnO nanoparticles as promising antimicrobial agents, especially for targeting Gram-positive bacteria and certain fungal pathogens, warranting further mechanistic and in vivo investigations (Babayevska et al., 2022; Sirelkhatim et al., 2015).

Conclusion

The blue-shifted UV–Vis peak and XRD results confirmed quantum confinement and a crystallite size near 25 nm. FTIR identified phytochemical groups that stabilized the particles, consistent with moderate colloidal stability and aggregation seen in DLS, zeta potential, and SEM data. Biologically, the nanoparticles exhibited strong antibacterial effects against *Staphylococcus aureus* selective antifungal action against *Trichoderma reesei*, and moderate

antioxidant activity. The phytochemical capping contributed to both particle stability and biological performance. Future research should explore molecular mechanisms, scalability, and biomedical applications, including targeted drug delivery and formulations against drug-resistant pathogens. Overall, the *Malva parviflora*-mediated biosynthesis of ZnO nanoparticles presents a robust, eco-friendly, and multifunctional nanomaterial platform poised for impactful translational research and innovative biomedical applications.

Reference

Abd-El-Rahim-Mashaly I (2012). Autecology and economic potentialities of Malva parviflora L. at El Dakahlia, Nile Delta. *J Environ Sci*, *42*, 661-683.

Abdelbaky A S, Abd El-Mageed T A, Babalghith A O, Selim S & Mohamed A (2022). Green Synthesis and Characterization of ZnO Nanoparticles Using Pelargonium odoratissimum (L.) Aqueous Leaf Extract and Their Antioxidant, Antibacterial and Anti-inflammatory Activities. *Antioxidants (Basel)*, *11*(8).

Abdullah F, Bakar N A & Bakar M A (2020). Low temperature biosynthesis of crystalline zinc oxide nanoparticles from Musa acuminata peel extract for visible-light degradation of methylene blue. *Optik*, *206*, 164279.

Ahmed T & Edvinsson T (2020). Optical Quantum Confinement in Ultrasmall ZnO and the Effect of Size on Their Photocatalytic Activity. *The Journal of Physical Chemistry C*, *124*(11), 6395-6404.

Akhtar M S, Panwar J & Yun Y-S (2013). Biogenic Synthesis of Metallic Nanoparticles by Plant Extracts. *ACS Sustainable Chemistry & Engineering*, *1*(6), 591-602.

Al-Hamad K A, Asiri A, Alqahtani A M, Alotaibi S Almalki A (2025). Monitoring the Antibacterial Activity of the Green Synthesized ZnO Nanoparticles on the Negative and Positive Gram Bacteria Mimicking Oral Environment by Using a Quartz Tuning Fork (QTF) Micromechanical Sensor. *Int J Nanomedicine*, *20*, 7975-7985.

Al-Qarawi K K & Al-Obaidi,H M R (2018). Detection of the active compounds in the leaves of the Common mallow plant Malva parviflora L. using GC-MS and HPLC technology. *Kufa Journal For Agricultural Sciences*, *10*(4).

Babayevska N, Przysiecka L, Iatsunskyi I, Nowaczyk G, Jarek M, Janiszewska E & Jurga S (2022). ZnO size and shape effect on antibacterial activity and cytotoxicity profile. *Sci Rep*, *12*(1), 8148.

Baliyan S, Mukherjee R, Priyadarshini A, Vibhuti A, Gupta A, Pandey R P & Chang C M (2022). Determination of Antioxidants by DPPH Radical Scavenging Activity and Quantitative Phytochemical Analysis of Ficus religiosa. *Molecules*, *27*(4).

Bhattacharjee S (2016). DLS and zeta potential - What they are and what they are not? *J Control Release*, *235*, 337-351.

Chauhan A K, Kataria N & Garg V K (2020). Green fabrication of ZnO nanoparticles using Eucalyptus spp. leaves extract and their application in wastewater remediation. *Chemosphere*, *247*, 125803.

Cheperli AM, Mokaber-Esfahani M, Taleghani A & Bahalkeh F (2024). Biosynthesis, characterization and antimicrobial activities of zinc oxide nanoparticles from leaf and seed extracts of Malva neglectaWallr. *Inorganic and Nano-Metal Chemistry*, *55*(6), 711-721.

Devatha C P & Thalla A K (2018). Green synthesis of nanomaterials. In *Synthesis of inorganic nanomaterials* (pp. 169-184). Elsevier.

Espitia P J P, Soares N d F F, Coimbra J S d R, de Andrade N J, Cruz R S & Medeiros E A A (2012). Zinc Oxide Nanoparticles:

Synthesis, Antimicrobial Activity and Food Packaging Applications. *Food and Bioprocess Technology*, *5*(5), 1447-1464.

Farhan H, Rammal H, Hijazi A & Badran B (2012). Preliminary phytochemical screening and extraction of polyphenol from stems and leaves of a Lebanese plant Malva parviflora L. *Int J Curr Pharm Res*, *4*(1), 55-59.

Forouzanfar F, Bazzaz B S & Hosseinzadeh H (2014). Black cumin (Nigella sativa) and its constituent (thymoquinone): a review on antimicrobial effects. *Iran J Basic Med Sci*, *17*(12), 929-938. https://www.ncbi.nlm.nih.gov/pubmed/25859296

Galstyan V, Comini E, Baratto C, Faglia G & Sberveglieri G (2015). Nanostructured ZnO chemical gas sensors. *Ceramics International*, *41*(10), 14239-14244.

Ganesh Saratale R, Kumar G, Banu R, Xia A, Periyasamy S & Dattatraya Saratale G (2018). A critical review on anaerobic digestion of microalgae and macroalgae and co-digestion of biomass for enhanced methane generation. *Bioresour Technol*, *262*, 319-332.

Hrishikesh Upadhyaya H U, Soumitra Shome S S, Rajdeep Sarma RS, Sujit Tewari S T, Bhattacharya, M, & Panda S (2018). Green synthesis, characterization and antibacterial activity of ZnO nanoparticles.

Huang J, Li Q, Sun D, Lu Y, Su Y, Yang X, Wang H, Wang Y, Shao W, He N, Hong J & Chen C (2007). Biosynthesis of silver and gold nanoparticles by novel sundriedCinnamomum camphoraleaf. *Nanotechnology*, *18*(10).

Hussien N A, Khalil M, Schagerl M & Ali S S (2025). Green Synthesis of Zinc Oxide Nanoparticles as a Promising Nanomedicine Approach for Anticancer, Antibacterial, and Anti-Inflammatory Therapies. *Int J Nanomedicine*, *20*, 4299-4317. https://doi.org/10.2147/IJN.S507214

Ijaz M, Zafar M, Islam A, Afsheen S & Iqbal T (2020). A Review on Antibacterial Properties of Biologically Synthesized Zinc Oxide Nanostructures. *Journal of Inorganic and Organometallic Polymers and Materials*, *30*(8), 2815-2826.

Iqbal T. Ara G, Khalid N & Ijaz M (2020). Simple synthesis of Ag-doped CdS nanostructure material with excellent properties. *Applied Nanoscience*, *10*(1), 23-28.

Iqbal T, Irfan F, Afsheen S, Zafar M, Naeem S & Raza A (2021). Synthesis and characterization of Ag–TiO2 nano-composites to study their effect on seed germination. *Applied Nanoscience*, *11*(7), 2043-2057.

Iravani S (2011). Green synthesis of metal nanoparticles using plants. *Green Chemistry*, *13*(10).

Javidan A, Ramezani M, Sobhani-Nasab A & Hosseinpour-Mashkani S M (2015). Synthesis, characterization, and magnetic property of monoferrite BaFe2O4 nanoparticles with aid of a novel precursor. *Journal of Materials Science: Materials in Electronics*, *26*(6), 3813-3818.

Jose B J A & Shinde M D (2024). Colloidal stability and dielectric behavior of eco-friendly synthesized zinc oxide nanostructures from Moringa seeds. *Sci Rep*, *14*(1), 2310.

Kedare S B & Singh R P (2011). Genesis and development of DPPH method of antioxidant assay. *J Food Sci Technol*, *48*(4), 412-422.

Kesharwani J, Yoon K Y, Hwang J & Rai M (2009). Phytofabrication of Silver Nanoparticles by Leaf Extract of <I>Datura metel</I>: Hypothetical Mechanism Involved in Synthesis. *Journal of Bionanoscience*, *3*(1), 39-44. https://doi.org/10.1166/jbns.2009.1008

Kumar S, Mohan M, Gandhimathi R & Amuda P (2009). Study on the anti-seizure activity of methanolic extracts of

Indigofera tinctoria (L). *Pharmacologyonline*, *1*, 1341-1351.

Le Nhat Trang N, Thi Nguyet Nga D, Tufa L T, Tran V T, Hung T T, Ngoc Phan V, Pham T N, Hoang V T & Le A T (2023). Unveiling the effect of crystallinity and particle size of biogenic Ag/ZnO nanocomposites on the electrochemical sensing performance of carbaryl detection in agricultural products. *RSC Adv*, *13*(13), 8753-8764. https://doi.org/10.1039/d3ra00399j

Li S, Shen Y, Xie A, Yu X, Qiu L, Zhang L & Zhang Q (2007). Green synthesis of silver nanoparticles using Capsicum annuum L. extract. *Green Chemistry*, *9*(8).

Li X, Xu H, Chen Z.S & Chen G (2011). Biosynthesis of Nanoparticles by Microorganisms and Their Applications. *Journal of Nanomaterials*, *2011*, 1-16.

Makarov V V, Love A J, Sinitsyna O V, Makarova S S, Yaminsky I V, Taliansky M E & Kalinina N O (2014). "Green" nanotechnologies: synthesis of metal nanoparticles using plants. *Acta Naturae*, *6*(1), 35-44.

Malik P, Shankar R, Malik V, Sharma N & Mukherjee T K (2014). Green Chemistry Based Benign Routes for Nanoparticle Synthesis. *Journal of Nanoparticles*, *2014*, 1-14.

Mendes C R, Dilarri G, Forsan C F, Sapata V M R, Lopes P R M, de Moraes P B, Montagnolli R N, Ferreira H & Bidoia E D (2022). Antibacterial action and target mechanisms of zinc oxide nanoparticles against bacterial pathogens. *Sci Rep*, *12*(1), 2658.

Miri A. Khatami M, Ebrahimy O & Sarani M (2020). Cytotoxic and antifungal studies of biosynthesized zinc oxide nanoparticles using extract of Prosopis farcta fruit. *Green Chemistry Letters and Reviews*, *13*(1), 27-33.

Mittal A K, Chisti Y & Banerjee U C (2013). Synthesis of metallic nanoparticles using plant extracts. *Biotechnol Adv*, *31*(2), 346-356. https://doi.org/10.1016/j.biotechadv.2013.01.003

Mukunthan, K. S., & Balaji, S. (2012). Cashew Apple Juice (Anacardium occidentaleL.) Speeds Up the Synthesis of Silver Nanoparticles. *International Journal of Green Nanotechnology*, *4*(2), 71-79.

Murray R D H, Méndez J & Brown,S A (1982). The natural coumarins.

Mustapha S, Ndamitso M M, Abdulkareem A S, Tijani J O, Shuaib D T, Mohammed A K & Sumaila A (2019). Comparative study of crystallite size using Williamson-Hall and Debye-Scherrer plots for ZnO nanoparticles. *Advances in Natural Sciences: Nanoscience and Nanotechnology*, *10*(4).

Noah N (2019). Green synthesis: Characterization and application of silver and gold nanoparticles. In *Green synthesis, characterization and applications of nanoparticles* (pp. 111-135). Elsevier.

Raliya R, Nair R, Chavalmane S, Wang W N & Biswas P (2015). Mechanistic evaluation of translocation and physiological impact of titanium dioxide and zinc oxide nanoparticles on the tomato (Solanum lycopersicum L.) plant. *Metallomics*, *7*(12), 1584-1594.

Şahin B, Soylu S, Kara M, Türkmen M, Aydin R & Çetin H (2021). Superior antibacterial activity against seed-borne plant bacterial disease agents and enhanced physical properties of novel green synthesized nanostructured ZnO using Thymbra spicata plant extract. *Ceramics International*, *47*(1), 341-350. https://doi.org/10.1016/j.ceramint.2020.08.139

Shehata H S & Galal T (2014). Phytosociology and phytochemical screening of the medicinal weed Malva parviflora. *Life Sci. J*, *11*(6), 458-468.

Singh A & Navneet D (2017). Ethnomedicinal, Antimicrobial and Pharmacological aspects of Malva parviflora Linn.: A review. *J. Phytopharmacol*, *6*, 247-250.

Singh,J, Dutta T, Kim K H, Rawat M, Samddar P & Kumar P (2018). 'Green' synthesis of metals and their oxide nanoparticles: applications for environmental remediation. *J Nanobiotechnology*, *16*(1), 84.

Sirelkhatim A, Mahmud S, Seeni A, Kaus N H M, Ann L C, Bakhori S K M, Hasan H & Mohamad D (2015). Review on Zinc Oxide Nanoparticles: Antibacterial Activity and Toxicity Mechanism. *Nanomicro Lett*, *7*(3), 219-242. https://doi.org/10.1007/s40820-015-0040-x

Song Z, Kelf T A, Sanchez W H, Roberts M S, Ricka J, Frenz M & Zvyagin A V (2011). Characterization of optical properties of ZnO nanoparticles for quantitative imaging of transdermal transport. *Biomed Opt Express*, *2*(12), 3321-3333.

Subba B, Rai G B, Bhandary R, Parajuli P, Thapa N, Kandel D R, Mulmi S, Shrestha S & Malla S (2024). Antifungal activity of zinc oxide nanoparticles (ZnO NPs) on Fusarium equiseti phytopathogen isolated from tomato plant in Nepal. *Heliyon*, *10*(22), e40198.

Sulak M (2021). Preparation of G-CuO NPs and G-ZnO NPs with mallow leaves, investigation of their antibacterial behavior and synthesis of bis(indolyl)methane compounds under solvent-free microwave assisted dry milling conditions using G-CuO NPs as a catalyst. *Turk J Chem*, *45*(5), 1517-1532.

Tomaszewska E, Soliwoda K, Kadziola K, Tkacz-Szczesna B, Celichowski G, Cichomski M, Szmaja W, Grobelny J & Yu W W (2013). Detection Limits of DLS and UV-Vis Spectroscopy in Characterization of Polydisperse Nanoparticles Colloids. *Journal of Nanomaterials*, *2013*(1). https://doi.org/10.1155/2013/313081

Wang Z L (2004). Zinc oxide nanostructures: growth, properties and applications. *Journal of Physics: Condensed Matter*, *16*(25), R829-R858.

Zhao L.-H, Zhang R, Zhang J & Sun S-Q (2012). Synthesis and characterization of biocompatible ZnO nanoparticles. *CrystEngComm*, *14*(3), 945-950. https://doi.org/10.1039/c1ce05621b